JAAS

ROYAL SOCIETY OF CHEMISTRY

PAPER

View Article Online
View Journal | View Issue

Cite this: J. Anal. At. Spectrom., 2022, 37, 1298

Effects of argon on the analytical properties of a microwave-sustained, inductively coupled, atmospheric-pressure plasma†

Helmar Wiltsche, *[a] Matthias Wolfgang [ab] and Franz Hallwirth[a]

The effects of argon added to a high-power microwave-sustained, inductively coupled, atmospheric-pressure plasma (MICAP) initially operated with nitrogen as the sole plasma gas were investigated. While replacing nitrogen in the intermediate gas flow with argon had negligible effects on the emission signal intensities of 65 emission lines of 29 elements, 100% argon in the nebulizer gas flow resulted in a line-dependent signal suppression of up to 70%. Pure argon in both the intermediate and nebulizer gas flows and nitrogen in the outer gas flow interestingly resulted in a signal enhancement of up to 60% for high excitation energy atom and ion lines. Moreover, limits of detection determined with this gas composition showed an improvement exceeding a factor of two for Na(I) 588.995 nm, Na(I) 589.592 nm, Ni(II) 231.604 nm, Sb(I) 206.833 nm, and Sb(I) 217.581 nm. On the other hand, the addition of argon to the outer gas stream was found to be problematic: above an argon fraction of 71%, the initially diffuse plasma discharge filamented into a thin, highly luminous ring. The MICAP could not be operated under these conditions over a prolonged time due to the expansion of the plasma ring towards the quartz torch wall and subsequent damage of the torch (melting). Argon was found to constrict the plasma core when added to the intermediate or outer gas flow. This constriction was followed by a widening of the analyte channel and a general loss in analyte emission intensity. The effect was largest for a mixed gas plasma with an outer gas stream composed of 71% argon and 29% nitrogen, showing a 60% increase of the analyte channel cross section diameter and a line-dependent emission line signal loss of 20 to 50%. Moreover, no combination of nitrogen/argon in either gas flow was found to significantly reduce the highly structured nitrogen plasma background of the MICAP. High-speed imaging revealed that the filamented plasma discharge is composed of several small plasma segments that chaotically rotate around the center of the plasma torus resulting in what is perceived to be a thin, highly luminous ring.

Received 4th February 2022
Accepted 19th April 2022

DOI: 10.1039/d2ja00036a

rsc.li/jaas

Introduction

Research on the application of microwave induced plasmas (MIPs) in analytical chemistry has been conducted for decades.[1] However, when it comes to the actual number of instruments used in routine laboratories, the inductively coupled plasma (ICP) is the dominating plasma source for both optical emission (ICP-OES) and elemental mass spectrometry (ICP-MS). Reasons for this are diverse, but the fact that limits of detection (LODs) in ICP-OES are about one order of magnitude lower compared to those in MIP-OES, even when using the same spectrometer,[2,3] should not be underestimated. While there are several ways of constructing a microwave-powered plasma source,[4] nitrogen has been commonly used as a plasma gas in high power (≥1000 W) MIPs rather than argon due to plasma filamentation – which is the collapse of a diffuse, toroidal discharge into an arc. In contrast to MIPs, ICPs are always operated with argon nowadays. This is advantageous due to the higher ionization potential of argon (15.7 eV for Ar *vs.* 14.5 eV for N_2), resulting in improved excitation and ionization of most elements. Moreover, the optical plasma background is significantly smaller and less structured in an argon plasma when compared to a nitrogen plasma.[3] All the above mentioned factors contribute to the degraded LODs of microwave-based plasma sources, operated with nitrogen as the plasma gas. While nitrogen is generally cheaper and can even be produced on-site from compressed air in a nitrogen generator, argon is preferred from an analytical point of view. It therefore might seem tempting to venture into the operation of MIPs with argon or mixtures of argon and nitrogen.

As early as 1951 Cobine and Wilbur[1] noted that microwave plasmas behave quite differently when using argon compared to molecular gasses such as nitrogen. While the latter showed flame-like discharges, argon produced elongated, filamentous

[a]Graz University of Technology, Institute of Analytical Chemistry and Food Chemistry, Graz, Austria. E-mail: helmar.wiltsche@tugraz.at

[b]Research Center Pharmaceutical Engineering GmbH, Graz, Austria

† Electronic supplementary information (ESI) available. See https://doi.org/10.1039/d2ja00036a

plasmas. In 2002, Moon and Choe systematically investigated argon as the plasma gas for a high power MIP.[5] They concluded that for a glass tube with 18 mm inner diameter (ID), flushed with 2.5–5 L min^{-1} Ar, under all investigated conditions a filament-like discharge was formed. These filaments consisted of thin, very bright, spatially unstable plasma strands.

By using a novel brass microwave plasma torch (MPT), Jin *et al.*[6] were able to maintain a stable argon MIP at power levels of up to 150 W. Due to the relatively low power, the argon consumption of this plasma source could be reduced to about 1 L min^{-1}. However, as noted by Barnes *et al.*[7] the MPT is less robust towards high solvent loads and can suffer from matrix effects. Another problem encountered when coupling the MPT to a mass spectrometer was degraded isotope-ratio accuracy and precision.

Okamoto *et al.*[8] constructed a high power microwave plasma source using argon as the plasma gas based on a narrow bore (2–4 mm ID) quartz discharge tube. Thereafter, an annular shaped plasma was formed in argon at 1300 W power. While LODs comparable to those of ICP-OES could be attained, the external cooling of the discharge tube posed a limit on the maximum microwave power and potentially the lifetime of the tube.

Jankowski *et al.*[9,10] further investigated the analytical properties of narrow bore discharge tube microwave plasmas using argon or argon/helium mixtures as the plasma gas at reduced power. Giersz *et al.*[11] extended this work and developed a microwave-driven ICP operated at atmospheric pressure using argon or helium as the plasma gas. This approach allowed the use of torch outer diameters of up to 20 mm facilitating the introduction of undesolvated sample aerosols generated by an ultrasonic nebulizer. As the used plasma torch was lacking an outer gas flow, the maximum power was however limited to about 300 W.

Moon and Choe[12] extended their investigation to the characteristics of an oxygen/argon plasma in 2006. They used again an 18 mm ID torch, quite similar to an ICP torch with the exception that no injector tube and consequently no inner gas stream were present. With oxygen as the outer gas flow and argon as the intermediate gas flow, they were able to form a stable, diffuse – which means not filamenting – discharge.

The filamentation phenomenon was further investigated by Cardoso *et al.* in 2009 using high-speed photography to study these filaments in argon.[13] They concluded that the number of filaments increases with increasing absorbed microwave power, discharge tube diameter and pressure. Moreover, Cardoso *et al.* found that the dimension of the filaments increased in a linear manner with the absorbed power.

Hong and Uhm[14] could show that the addition of a small amount of a molecular gas is able to suppress plasma filamentation in argon. At 1000 W additions of 0.3% CH_4 or 0.4% CO_2 or 0.8% O_2 or 1% N_2 were found to be sufficient. The authors concluded that the different thermal conductivities of the investigated gasses are the main reason for the differences in the required amounts of these molecular gasses. From a mechanistic point of view, Hong and Uhm assumed molecular gasses to suppress plasma filamentation because of two conditions that have to be fulfilled simultaneously: first, molecular gasses increase the gas kinetic temperature due to their higher thermal conductivity compared to argon and second, they reduce the electron density in the filaments. Following these findings, Castaños-Martínez *et al.*[15] found that not only small amounts of molecular gasses can suppress plasma filamentation in argon, but also noble gasses with an ionization energy lower than that of argon *e.g.* krypton and xenon. They obtained a diffuse plasma discharge when adding either 0.5% Kr or 0.07% Xe. The authors additionally noted that metastable atoms seem to contribute to the stabilization of a diffuse argon plasma. Clearly, the assumptions of Hong and Uhm[14] cannot provide sufficient explanation for the observations of Castaños-Martínez and coworkers, as small additions of Kr or Xe will not appreciably change the overall thermal conductivity of the bulk plasma gas flow.

While the operation of high power MIPs using only argon as the plasma forming gas is challenging, nitrogen/argon mixtures seem to be a viable alternative. In fact, there is an interesting similarity of this approach to the ICP: while ICPs are nowadays operated exclusively with argon as the plasma forming gas, the addition of nitrogen has been reported to be beneficial in certain cases. For ICP-MS, Louie and Soo[16] demonstrated that the addition of small quantities (about 0.2%) of nitrogen to all gas streams of the plasma torch resulted in a decrease of both oxygen based polyatomic interference and doubly charged ions as well as a general increase of the sensitivity throughout the mass range by a factor of 2–5. Similar observations were made by Hu *et al.*[17] for laser ablation ICP-MS. Agatemor and Beauchemin[18] showed that the addition of small quantities (about 0.1% v/v) of nitrogen to the outer- and inner gas flows minimizes the matrix effects of sodium in solution nebulization ICP-MS, while improving the LODs of Al, Co, Pd, and V. The concept of argon/nitrogen mixed gas plasmas is also well known in ICP-OES; Montaser and Mortazavi[19] showed that a stable plasma discharge can be maintained with up to 100% nitrogen in the outer gas flow of a conventional ICP (Fassel-type) torch without the need for excessively high plasma power (>5 kW) as used in previous approaches by Greenfield and Smith.[20] While argon/nitrogen mixed gas ICPs are smaller in size and require lower radial observation heights, the attained LODs for a number of elements were higher when compared to those of an all-argon ICP. A similar observation was made by Meyer and Barnes[21] for an ICP operated with nitrogen as the sole plasma forming gas. Ohata[22] further studied the effect of up to 6% (v/v) nitrogen in the outer gas flow of an axially viewed ICP-OES and also encountered nitrogen-induced shrinking of the plasma. The LODs of some high energy atom lines (As, Bi, P, S and Zn) and ion lines (Cd, Fe, Ni, and Zn) could be improved by a factor of 2–7 due to the addition of nitrogen, whereas for most other emission lines an increase of the LOD was encountered when compared to that of a standard argon-only ICP-OES. Scheffler and Pozebon[23] introduced small quantities (<3% v/v) of nitrogen into the inner (nebulizer) gas flow of an axially viewed ICP-OES. The authors found that nitrogen increased the plasma robustness[24] by up to 50%. Moreover, a considerable reduction of the matrix effects of high concentrations of Na, K and Ca by nitrogen on a number of emission lines was reported.

While from the mechanistic point of view, the filamentation of argon-based microwave plasmas is well documented, implications on the analytical capabilities are scarcely discussed in the literature. Particularly, MIP properties at the brink of filamentation are largely unexplored. As krypton and xenon are too expensive for routine laboratories even when consumed only at flow rates of a few ml min^{-1}, this work focuses on argon/nitrogen mixed gas microwave plasmas, extending our previous work on air as the plasma gas.[3] As already noted, the use of nitrogen as the plasma gas entails an intense, highly structured optical plasma background over most of the spectrum relevant for optical emission spectrometry as well as degraded analyte excitation and ionization when compared to an argon ICP. Clearly, any improvement of one or both shortcomings of nitrogen plasmas can be expected to narrow the gap between MIPs and ICPs in terms of LODs. As nitrogen is the root cause of the degraded performance, but a pure argon high power MIP is not feasible due to filamentation, the admixing of argon to an initially pure nitrogen MIP is investigated. A high-power microwave-sustained, inductively coupled, atmospheric-pressure plasma (MICAP) is used under high-speed imaging surveillance to investigate the effect of the plasma gas composition on LODs.

Experimental

Instrumentation

A microwave-sustained, inductively coupled, atmospheric-pressure plasma (MICAP) source[25] was coupled to the simultaneous spectrometer of a commercial ICP-OES (Ciros Vision EOP, Spectro, Germany), as illustrated in Fig. 1.[3] The microwave energy was provided by a 2M262A 1.5 kW 2.45 GHz magnetron connected to a Magdrive 2000 (Dipolar AB, Sweden) high voltage power supply. A conventional one-piece ICP-OES torch (for Ciros Vision EOP, Spectro, Germany) having the following dimensions was used: outer quartz glass tube: 17 mm inner diameter (ID), 19.4 mm outer diameter (OD); intermediate quartz tube: 14 mm ID, 16 mm OD, injector tube: 2.5 mm ID, 6 mm OD. While the nitrogen supply to the MICAP torch was adjusted *via* an external control unit (Radom Corp., USA), argon was controlled by the mass flow controllers of the ICP-OES instrument, whose spectrometer was used for this work. The sample introduction system comprised a standard baffled cyclonic spray chamber (Glass Expansion, Australia) and a glass concentric nebulizer (Type A, Meinhard, USA).

For high-speed imaging, a 3-megapixel camera, capable of acquiring up to 200 000 frames per second (fps) (MotionBLITZ EoSens mini2, Mikrotron, Germany), was used. Plasma images (144 × 150 pixel) were directly recorded in axial plasma viewing with a Kowa LM35 ($f = 35$ mm/F1.4, used at f-number 4) objective using 62 μs exposure time resulting in 15 000 fps temporal resolution. No additional light absorbing filters were used. The image conversion factor was determined photogrammetrically to be 118 μm per pixel. It is important to note that for imaging experiments the MICAP was detached from the spectrometer allowing axial plasma viewing by the high-speed camera. To avoid microwave radiation leakage to the laboratory environment during these high-speed imaging experiments, a grounded aluminum attenuation tube (40 mm inner diameter, 80 mm long) was attached to the front face of the MICAP source.

Standard operating conditions used throughout all experiments are listed in Table 1. The only exceptions are high-speed imaging investigations, where the microwave power was reduced to 1000 W, in order to prevent serious torch damage during plasma filamentation. It is important to note that at 1500 W similar observations to the case of 1000 W microwave power were made visually.

Reagents

Purified water (18 MΩ cm, Barnstead Nanopure, Thermo Fisher Scientific, USA) and high purity nitric acid (Roth, Germany, purified by subboiling) were used throughout. Standard solutions were prepared from a 100 mg L^{-1} multi-element stock solution (Al, As, B, Ba, Be, Bi, Ca, Cd, Co, Cr, Cu, Fe, K, Li, Mg, Mn, Mo, Na, Ni, Pb, Sb, Se, Sr, Ti, Tl, V, and Zn, Roth, Germany), 1 g L^{-1} single element stock solutions (As, B, Bi, S, Se, P, Pb; Roth, Germany) or 10 g L^{-1} single element stock solutions (Fe, Alfa Aesar, Germany) by dilution with 3% HNO_3 (v/v). Argon (5.0 quality, Messer, Austria) and nitrogen (5.0 quality, boil-off from a liquid nitrogen storage tank, Linde, Austria) were used.

Experimental procedure

In order to record a consistent set of data, the effects of argon added to the three gas streams of the MICAP plasma torch were investigated using a standardized procedure with four test standards: blank solution: (3% v/v nitric acid); solution #1:

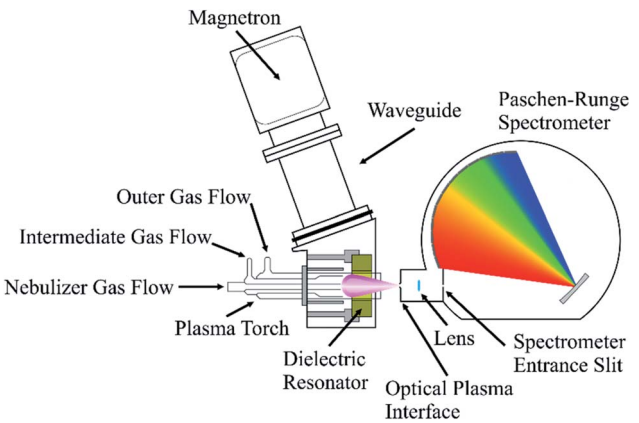

Fig. 1 Top view diagram of the MICAP attached to the simultaneous spectrometer of the used ICP-OES.

Table 1 Instrument operating conditions for the MICAP

Parameter	MICAP
Power, W	1500
Outer gas flow, L min^{-1}	16
Intermediate gas flow, L min^{-1}	0.6
Nebulizer gas flow, L min^{-1}	0.85
Integration time, s	24 (full spectrum)
Replicates	5

2 mg L^{-1} of Al, Ba, Be, Ca, Cd, Co, Cr, Cu, Fe, K, Li, Mg, Mn, Mo, Na, Ni, Sb, Sr, Ti, Tl, V, and Zn, 12 mg L^{-1} of B, Bi, and Pb, and 22 mg L^{-1} As and Se in 3% v/v nitric acid; solution #2: 50 mg L^{-1} of P and S in 3% v/v nitric acid; solution #3: 400 mg L^{-1} Fe in 3% v/v nitric acid.

Between these four solutions, the sample introduction system was rinsed with diluted nitric acid (3% v/v) for 90 seconds. For the sake of clarity, emission intensities of each line were normalized to the intensity in a pure nitrogen plasma by dividing the background corrected intensities recorded in the presence of varying amounts of argon by the background corrected emission intensity of the line in a pure nitrogen plasma. Therefore any enhancement or suppression by argon can be easily identified. The line selection was based on previous work on MICAPs in axial viewing.[3]

The excitation temperature T_{exc} was calculated from the slope of a Boltzmann plot[26] of 22 Fe(I) emission lines located in the spectral region ~367–377 nm. Emission signals of the 400 mg L^{-1} Fe solution (solution #3) were used for this purpose.

Due to differences in the spectral response of the individual CCD detector chips installed in the simultaneous spectrometer, only Fe(I) emission lines located on a single CCD detector chip were selected. Wavelengths and the used fundamental constants[27,28] are listed in ESI Table S1.†

LODs and LOQs were determined for 29 elements using a total of 63 emission lines. The calibration range was covered by eight equidistant standards. For As, Bi, and Se the concentration range was 0.22–1.54 mg L^{-1}, for S and P 0.1–5.0 mg L^{-1} and for all other elements 0.02–0.14 mg L^{-1}. LODs were calculated by the blank method and LOQs were calculated using the calibration method,[3] applying the instrumental conditions listed in Table 1. Details of the calculation procedures can be found in the study by Hesse *et al.*[29]

Image processing

Images recorded with a high-speed camera were exported from the cameras raw data stream to a lossless *tif format and 3000 images (equal to a time segment of 200 ms) were averaged for each experiment using the freeware Fitswork (Fitswork 4.47, **https://www.fitswork.de**) in order to gain a fluctuation free 16 bit grayscale image. These images were further analyzed using the free image manipulation software GIMP (GIMP v2.10.20, **https://www.gimp.org**). The image parts containing the plasma (defined by the inner cross section of the torch) were cut out (102 × 102 pixels) and subsequently a "posterization" filter was applied. This filter reduces the amount of grayscale values to 4 defined equidistant levels distributed over the whole dynamic range of 16 bits. Therefore, different areas of interest (plasma ring and analyte channel) in the original images are highlighted and can be evaluated in a standardized photogrammetrical manner.

Results and discussion

Effect of argon on the nitrogen plasma discharge

Initial experiments were conducted to evaluate the effect of argon on the MICAP. Particularly the onset of filamentation was found to be troublesome, as the plasma discharge tends to expand towards the wall causing torch damage. Contrary to previously reported microwave discharges,[1,5,12,13] the MICAP does not form long, arc-like filaments but rather a thin, highly luminous ring. This ring is located in close proximity to the inner wall of the torch outer glass tube – a region that is commonly occupied by the outer gas flow. Consequently, the formation of this ring filament created a loud, hissing noise due to the shearing of the plasma ring by the outer gas stream. It should be noted that the MICAP could not be operated for more than a few seconds under these conditions, before the torch was damaged by melting of the outer tube.

A comparison between the diffuse plasma of the MICAP using nitrogen as the sole plasma gas and the highly luminous plasma filament in the presence of large quantities of argon is shown in Fig. 2. From this figure it is also apparent that under standard operating conditions such as the ones listed in Table 1 using only nitrogen as the plasma gas, the MICAP does not expand towards the torch quartz glass wall, leaving enough space for the outer gas flow for efficient torch cooling.

The effect of argon on the initially pure nitrogen MICAP was studied by admixing argon to each gas stream separately, replacing some or all of the nitrogen but leaving the total gas flow constant. Initial experiments showed that the presence of argon in the nebulizer- and intermediate gas flows did not compromise the plasma stability noticeably. However, above about 71% argon in the outer gas flow, filamentation of the plasma discharge was observed.

In general, a widening of the region commonly associated with the analyte channel (in the center of the axially viewed plasma discharge) was encountered, when argon was admixed to the intermediate and outer gas flows, while no such effect was observed even for 100% argon in the nebulizer gas flow. As the widening was largest for argon addition to the outer gas flow, the quantification of this effect by high-speed imaging combined with photogrammetry will be exemplarily elaborated for this gas configuration. It is important to note that the same calculations were carried out for all mixtures of argon and nitrogen in the three gas flows of the MICAP torch. All these results are summarized in ESI Table S2† for the sake of completeness.

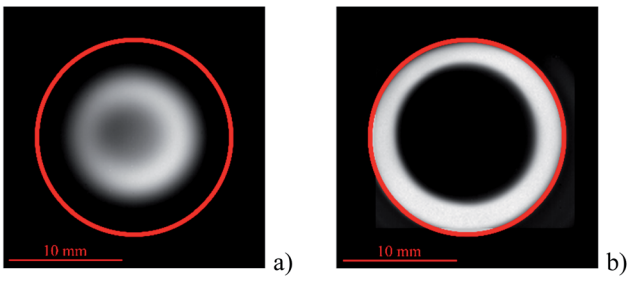

Fig. 2 Axial views (3000 high-speed images averaged) of the MICAP. (a) 100% nitrogen in all three gas streams (b) filamentation of the MICAP due to 100% argon in the outer gas stream (100% nitrogen in the intermediate and nebulizer gas streams). The red circle in both images illustrates the position and size of the quartz torch outer tube with respect to the plasma discharge.

In Fig. 3 the effect of an increasing concentration of argon in the outer gas stream of the MICAP discharge is shown, while pure nitrogen was fed to the intermediate and nebulizer gas flows. Up to 71% argon in the outer gas flow, the plasma structure remained fundamentally unchanged: a luminous but diffuse plasma core always surrounded the analyte channel. When comparing Fig. 3a with Fig. 3c, it becomes obvious that the luminous, diffuse plasma-ring became thinner with increasing argon concentration in the outer gas flow and thereby, the analyte channel considerably widened.

It is important to note that in Fig. 3a and c 3000 detector pictures corresponding to 200 ms total observation time were averaged to overcome image distortion by plasma streaks – this effect is discussed below. In order to obtain quantitative information from the plasma pictures, 3000 high-speed camera images of each experiment were split into 5 groups of 600 images each. Then for each group the images were averaged and afterwards the pixel gray scale information was reduced (as described above) to 4 levels. This procedure was selected to assess the signal variability over time for a given gas composition. Fig. 3b and d show that by posterization the analyte channel can be separated well from the surrounding plasma. Please note that the high-speed camera was slightly off-axis with respect to the MICAP discharge (approximately 5°) to avoid damage to the camera by the hot exhaust gasses. This resulted in a non-circular brightness distribution in the original images and a plasma core which thereby appears not to fully encircle the analyte channel.

The four level grayscale pictures in Fig. 3 and the results in ESI Table S4† qualitatively show a proportional widening of the analyte channel with increasing argon concentration in the outer gas flow. Quantitative information can be derived from these images by summing all pixels of the analyte channel and normalizing the corresponding pixel area of each N_2/Ar mixture to the area of pure nitrogen as shown in Fig. 4. It is interesting to note that up to 43% argon in the outer gas flow, no significant change in the analyte channel diameter was observed. Higher concentrations of argon however led to channel widening, resulting in a significant analyte channel area increase. At the maximum permissible argon concentration of 71% in the outer gas flow and pure nitrogen in the intermediate and nebulizer gas flows, the analyte channel was found to be widened by 51 ± 3% when compared to a pure nitrogen MICAP.

A similar, but less pronounced effect was observed for the intermediate gas flow, when nitrogen was gradually replaced by argon, while maintaining pure nitrogen in the nebulizer- and outer gas flows. In this case, the analyte channel also widened linearly with increasing argon concentration. At 100% argon in the intermediate gas flow, the analyte channel area increased by 15 ± 4% compared to that of a pure nitrogen MICAP.

As noted above, argon in the nebulizer gas flow had no measurable effect on the analyte channel. Even at 100% Ar in this gas flow, no significant change in the analyte channel area was encountered.

The addition of argon to more than one gas stream at the same time was investigated as well. With 100% argon in the nebulizer- and intermediate gas flows and 100% nitrogen in the outer gas flow, the analyte channel area increased only by 7 ± 3% compared to that in a pure nitrogen MICAP. Clearly, the presence of argon in the nebulizer gas stream slightly but significantly reduced the effect of argon in the intermediate gas

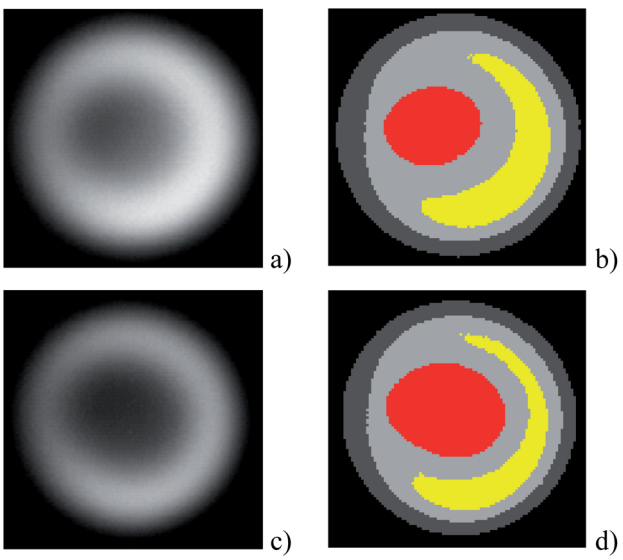

Fig. 3 Effect of argon concentration in the outer gas flow of a MICAP (1000 W microwave power; 0.9 L min^{-1} N_2 nebulizer gas flow, 0.6 L min^{-1} N_2 intermediate gas flow; 14 L min^{-1} N_2/Ar outer gas flow); the position of the camera and the magnification remained unchanged for all images. Gas composition in (a) and (b): 100% N_2 in the outer gas flow, whereas in (c) and (d) 29% N_2 + 71% Ar. For images (a) and (b) 3000 detector pictures were averaged. In images (c) and (d) the initial 16 bit (65 536 levels) grayscale information for the averaged images was reduced to 4 levels to better visualize the increasing size of the analyte channel at the center of the discharge. Color coding in images (b) and (d): red – analyte channel, yellow – most luminous part of the plasma core.

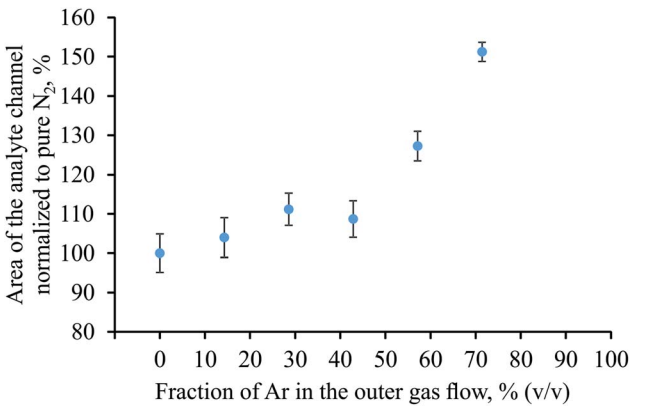

Fig. 4 Change of the visible analyte channel area observed in axial viewing as a function of the argon concentration in the outer gas flow. Data have been normalized to pure nitrogen for comparison. 600 detector images were pixel-averaged for one replicate prior to reduction to 4 grayscale levels for separating the analyte channel from the plasma core; $n = 5$; corresponding plasma images of the grayscale reduced versions are listed in ESI Table S4.†

flow, resulting in a widening of the analyte channel area of 7 ± 3% rather than 15 ± 4% as in the case of 100% argon in the intermediate gas flow and pure nitrogen in the nebulizer- and outer gas flows. As shown later, the combination of 100% argon in the nebulizer- and intermediate gas flows and pure nitrogen in the outer gas flow was found to enhance the emission signal of most of the investigated analyte lines, appearing to be the best combination for the investigated mixed gas MICAP.

An increased concentration of argon in the outer gas flow was also investigated with 100% argon in the intermediate and nebulizer gas flows. It is interesting to note that plasma filamentation occurred above 71% argon in the outer gas flow, irrespective of whether the intermediate and nebulizer gas flows were composed of argon or nitrogen. This might be explained by the fact that the outer gas flow represents the bulk of the total gas flow in the plasma torch. As a consequence, the composition of the outer gas flow will dominate the gas composition of the toroidal plasma core of the MICAP.

For 100% argon in the intermediate and nebulizer gas flows and an increasing concentration of argon in the outer gas flow a similar pattern to the case in Fig. 4 (pure nitrogen in the intermediate and nebulizer gas flows and an increasing concentration of argon in the outer gas flow) was encountered: while below 43% argon in the outer gas flow no significant change of the analyte channel cross section was encountered, above this concentration the analyte channel area linearly widened. At the maximal permissible argon concentration of 71%, the analyte channel cross section was 61 ± 3% larger than in the case of a pure nitrogen MICAP. Therefore, argon in the nebulizer- and intermediate gas flows caused some additional 10% increase in the analyte channel area over nitrogen in these two streams. It is important to note that although the analyte channel cross section did widen significantly with increasing argon concentration in the outer gas flow, the filamentation of the MICAP to a thin, bright ring is an abrupt event. It was not possible to obtain a stable plasma discharge with an analyte channel area larger than the noted 161% without immediate plasma filamentation.

Effect of argon on the analyte signal intensities of a nitrogen MICAP

While high-speed imaging provided insights into the effect of argon on the size of the analyte channel cross section, the analytically relevant implications on emission line signals were determined by emission spectrometry. For this purpose, emission spectra of two multi-element solutions containing a total of 29 elements were recorded for varying concentrations of argon in the three gas flows of the torch.

Beside the change in emission intensity, the excitation temperature calculated from iron atom lines, as well as the intensity ratio of the Mg(II) 280.270 nm and Mg(I) 285.21 nm emission lines was used to assess changes in the MICAP caused by argon. The Mg ion to atom line ratio, often referred to as "plasma robustness", is commonly used in ICP-OES to identify matrix effects or optimize plasma conditions.[24,30] It is important to note that for an argon ICP a magnesium ion to atom line ratio larger than 10 indicates a robust plasma. However, this number must not be directly applied to nitrogen plasmas such as MICAPs, as the electron number density and LTE plasma temperature differ considerably between a MIP and ICP: while for a resonant cavity MIP, electron number densities of 1.6 × 10^{19} m^{-3} to 2.7 × 10^{19} m^{-3} and an excitation temperature of about 5000 K have been reported,[31] typical values of electron number densities and excitation temperatures for an ICP are 5 × 10^{20} m^{-3} to 5 × 10^{21} m^{-3} and about 8000 K, respectively.[24] Therefore, plasma robustness values between 0.5 and 1.8 are to be expected for MIPs operated with nitrogen according to Chalyavi *et al.*,[31] who obtained values between 0.4 and 0.6 for a resonant cavity MIP at 1000 W microwave power. Thaler *et al.*[32] found values up to 1.8 under radial viewing for a MICAP at 1500 W. In the presented work, a plasma robustness of 1.6 was obtained at 1500 W for a pure nitrogen MICAP in axial viewing, which is expected and in agreement with the cited literature.

An overview of the effects of argon on the emission intensities of 60 emission lines from 29 elements investigated is visualized in Fig. 5. Numerical values with detailed line designations are provided in ESI Table S2.† Please note that in Fig. 5 only "extreme" gas conditions are shown, while in ESI Table S2† intermediate steps for each gas mixture are reported.

Addition of argon to the nebulizer gas flow. The addition of argon to the nebulizer flow provoked a signal suppression for most investigated emission lines as indicated in Fig. 5a. A more detailed view of the data listed in ESI Table S2† reveals that the addition of 44% (v/v) argon to the nebulizer gas flow leads to signal suppression in the range of 40% to 80% for all investigated elements with the exception of the alkaline metals Na and K. When the argon concentration in the nebulizer gas flow was further increased to 100%, all emission lines showed a corresponding increase in the emission intensity compared to 40% argon. However, with the exception of Li, Na, K, P and S no other element reached the same emission intensity as acquired in a pure nitrogen plasma. This suppression behavior is most interesting, indeed. The slight enhancement of the alkaline elements in the presence of argon might indicate a cooler normal analytical zone (NAZ), as this fosters an increase in the number of alkaline atoms in the ground state. However, there is no clear trend in the dataset which might link the total line energy to the level of suppression. All investigated emission line intensities of S and P obtained for pure nitrogen as well as for 100% argon in the nebulizer gas stream remained unchanged. This fact is surprising, as with the exception of the aforementioned alkaline elements, all other emission lines were suppressed by the presence of argon. In addition, the plasma background remained highly structured irrespective of the nebulizer gas flow composition. Changes in the signal intensity were therefore not caused by a change of the plasma background but rather by differences in the excitation conditions. It should be noted that the highly structured plasma background intensity remained in fact unchanged.

The excitation temperature seems to support the hypothesis of a slightly cooler NAZ: while in a pure nitrogen MICAP the excitation temperature was 5200 ± 100 K, it slightly decreased to 4700 ± 200 K at 44% argon in the nebulizer gas flow and

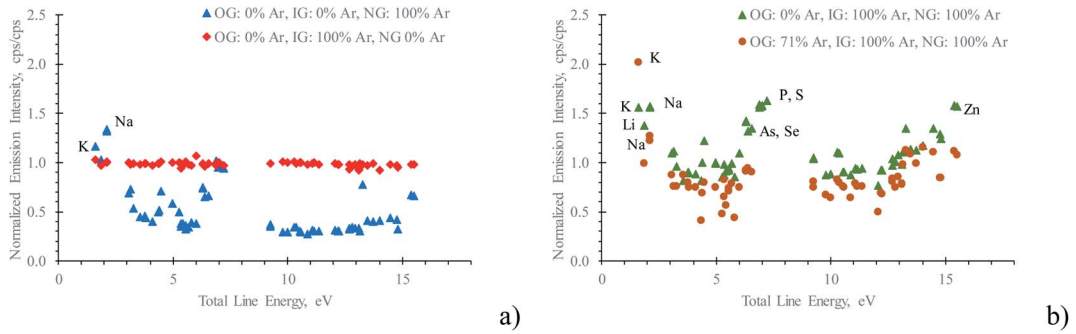

Fig. 5 Effect of the plasma gas composition on the normalized emission line intensity of 29 elements (60 emission lines) as a function of the total line energy (atom lines: excitation energy; ion lines: ionization energy + excitation energy). Gas composition in (a): 100% argon in the nebulizer- (NG) or intermediate gas (IG) flows and pure nitrogen in the other gas (OG) flows. Gas composition in (b) 100% argon in the intermediate and nebulizer gas flows and either pure nitrogen or an Ar/N_2 mixture with 39% (v/v) nitrogen in the outer gas flow. Please note that all underlying datasets plotted in this graph are listed in ESI Table S2.† RSDs < 2% for all lines; $n = 5$. Elements of special interest have been highlighted with the element symbol but the wavelength was omitted for clarity. Note that above 9 eV only ion lines are shown.

remained unchanged (4800 ± 100 K) when the argon fraction in this gas stream was increased to 100%. Unfortunately, the used spectrometer does not cover the spectral interval necessary to determine the electron number density from the Stark broadening of the H_β line. Lacking this essential information, it can only be concluded that argon in the nebulizer gas flow reduces the emission intensity of nearly all observed elements, with the exception of Li, Na, K, P and S. While the addition of argon to the nebulizer gas flow caused no significant change in the analyte channel diameter, the plasma robustness decreased from 1.6 for a pure nitrogen MICAP to about 0.9 at 44% argon in the nebulizer gas flow following the trend of all investigated emission lines with the exception of Na and K. At 100% argon in the nebulizer gas flow, a small increase in the plasma robustness to 1.0 was encountered. Again, most other investigated emission lines followed this trend and showed higher signals than at 44% argon in the nebulizer gas flow.

Addition of argon to the intermediate gas flow. Adding argon to the intermediate gas flow had no significant effect (<5%) on all investigated emission lines as shown in Fig. 5a and summarized in ESI Table S2.† This even holds true for 100% argon in the intermediate gas flow. While the analyte channel cross section area widened slightly by 15 ± 4%, no change in the excitation temperature or the plasma robustness was encountered when compared to a pure nitrogen MICAP. This might be explained by the fact that the intermediate gas flow has the smallest contribution (3.4% v/v) to the total gas flow of 17.5 L min^{-1} fed to the plasma torch and is furthermore not in direct contact with the sample aerosol.

Addition of argon to the nebulizer and intermediate gas flows. Replacing nitrogen in both the nebulizer and intermediate gas flows resulted in an enhancement of some emission lines compared to a nitrogen-only MICAP; as shown in Fig. 5b, the alkaline elements were enhanced by some 40–60%, but also for high excitation energy atom lines (>6 eV) of As, P, S and Se increased signals (30% to 60%) were observed. Above about 12 eV total line energy, all ion lines experienced a nearly linear enhancement with increasing line energy (10% to 60%) with the two zinc ion lines Zn(II) 202.548 nm and Zn(II) 206.191 nm showing the largest signal gain of 60% over a nitrogen-only MICAP. The excitation temperature under these conditions was similar to that of a pure nitrogen MICAP (5200 ± 100 K), while the plasma robustness slightly decreased to 1.5. It is interesting to note that Mg(II) 280.270 nm and Mg(I) 285.21 nm were both suppressed (77% and 81% of the signal intensity of a pure nitrogen MICAP) with 100% argon in the nebulizer and intermediate gas flows, while no signal change was encountered when argon was only introduced into the intermediate gas flow. Unexpectedly, magnesium experienced the largest suppression of all investigated elements when intermediate and nebulizer gas streams consisted of 100% argon. The analyte channel cross section area slightly, but significantly increased by 7 ± 3% compared to that observed for a pure nitrogen plasma. Again, the plasma background remained highly structured even when 100% argon was introduced in both intermediate- and nebulizer gas streams.

Addition of argon to the nebulizer, intermediate and outer gas flows. Pure argon in the nebulizer- and intermediate gas flows was generally found to be beneficial, as it enhanced the emission of high energy lines. However, if also in the outer gas flow the fraction of argon in the total gas flow was increased from 0% to 71%, all emission lines were suppressed by 20% to 50% (median of all lines: 30% suppression) when compared to the signals obtained with argon in the nebulizer- and intermediate gas streams and nitrogen in the outer gas stream as shown in Fig. 5b. The only exception was K(I) 766.491 nm. It is important to note that above 71% argon in the outer gas flow, the plasma was visually distorted and could not be operated for a prolonged period of time without filamentation to a ring discharge. At 71% argon in the outer gas flow, the excitation temperature remained at 5200 ± 100 K while the plasma robustness increased to 1.8 and the analyte channel cross section area reached the largest encountered area, increasing to 161 ± 3% compared to that of an all nitrogen plasma.

The widening of the analyte channel is a result of a constriction of the plasma torus. While its outer diameter

remained constant, its inner diameter increased with increasing concentration of argon in the outer gas flow. Therefore the sample aerosol can be expected to expand into a wider analyte channel, resulting in a less dense radiation source. Consequently, the encountered emission signal loss can be explained by the fact that the spectrometer entrance optics collects light only from a small but constant fraction of the analyte channel center. If in this zone the number of emitting species is reduced, an overall signal loss is to be expected. Moreover, species at the center of the analyte channel will be less effectively excited once the distance to the hot plasma torus increases, giving rise to a line-specific change in the emission intensity. The considerable increase in the plasma robustness from 1.6 in an all-nitrogen MICAP to 1.8 in a "mostly argon" MICAP can be interpreted with a shift in the ionization equilibrium; while the absolute signal intensities of both the atom and ion lines of magnesium decreased by more than 50% when compared to those of a pure nitrogen MICAP, their ratio changed. As the excitation temperature was similar for both, the all-nitrogen MICAP and the "mostly argon" MICAP, the increase in plasma robustness points to an increase in the electron number density. Chalyavi *et al.*[31] concluded from similar electron- and excitation temperatures of a resonant cavity MIP that a local thermal equilibrium is also present in all-nitrogen MIPs. This is an important prerequisite for the assumption that large quantities of argon increase the electron number density in the MICAP. However, the excitation temperature reported in this work is an averaged temperature over the small plasma volume segment imaged by the entrance optics on the spectrometer entrance slit. The fact that the excitation temperature did not markedly change with different argon concentrations in the three gas flows of the plasma torch indicates that for further plasma diagnostics radially resolved excitation temperatures are required. Nevertheless, the obtained excitation temperature for an all-nitrogen MICAP at 1500 W of 5200 ± 100 K is in good agreement with radial measurements by Thaler *et al.*,[32] who obtained 5200 ± 300 K for a MICAP at the same power level.

LOD/LOQ: comparison between a pure nitrogen and argon/nitrogen MICAP

As the highest signal enhancements were encountered for a MICAP with argon in the nebulizer- and intermediate gas flows and nitrogen as the outer gas flow, LODs and LOQs for several emission lines were determined for this setup. As exemplarily shown in Table 2 for selected emission lines, the overall improvement was rather small. Please note that a full list with 62 emission lines of 29 elements is given in ESI Table S3† providing the LOD and LOQ for all investigated lines. A decrease of the LOD by more than a factor of two was only encountered for Na(I) 588.995 nm, Na(I) 589.592 nm, Ni(II) 231.604 nm, Sb(I) 206.833 nm, and Sb(I) 217.581 nm. Clearly, the effect of argon on improving the LOD of a MICAP is small at best. It should be noted that with the exception of Na(I) 588.995 nm all other emission lines that showed improved LODs in an argon/nitrogen mixed gas MICAP were not the most sensitive lines of the respective elements.

Table 2 Limits of detection (LOD) calculated by the blank method of selected emission lines determined with a pure nitrogen or mixed-gas MICAP (pure argon in nebulizer- and intermediate gas flows; pure nitrogen in the outer gas flow)

	N_2 MICAP	Ar/N_2 MICAP
Element, emission line	LOD, μg L^{-1}	LOD, μg L^{-1}
Al(I) 396.152 nm	1	6
B(I) 249.773 nm	8	4
Ca(II) 393.366 nm	0.2	0.2
Cd(I) 228.802 nm	10	3
Cu(I) 324.754 nm	4	6
Fe(II) 259.941 nm	4	6
K(I) 766.491 nm	1	9
Mn(II) 259.373 nm	1	2
Na(I) 588.995 nm	5	0.4
Na(I) 589.592 nm	5	1
Ni(I) 352.454 nm	60	40
Ni(II) 231.604 nm	100	50
P(I) 213.618 nm	400	200
Pb(I) 405.778 nm	20	30
Sb(I) 206.833 nm	300	100
Sb(I) 217.581 nm	200	90
Zn(I) 213.856 nm	20	20

High-speed imaging: plasma streaks

During high-speed imaging experiments of plasma filamentation, fast moving streaks were encountered in the MICAP. These streaks appear to be formed in the outer regions of the plasma and travel through the MICAP similar to waves, also passing through the analyte channel. Fig. 6 shows a single frame (62 μs exposure time) of the high-speed camera video stream. The plasma is distorted at the outer surrounding and also at the center of the analyte channel a wave-like structure can be observed. A high-speed video showing these streaks is available (ESI: Plasma_streaks.mp4).† It is interesting to note that these streaks appear to be very fast: from the plasma video stream, it was determined that within 682 μs a streak passed through half of the plasma discharge of 12 mm diameter (calculated by photogrammetry). This results in a streak propagation speed of about 9 m s^{-1}. In this context it is important to note that the observed streaks are not an artefact caused by shimmering of hot gasses. The streaks are too fast for such an alternative explanation and the selected depth-focus of the used camera objective will exclude colder, less luminous zones outside the plasma core. The streaks have only been observed when focusing on the plasma core and do not occur in the plasma tail flame. Moreover, the hot plasma gasses were removed by a fume extraction hood installed above the horizontally orientated plasma torch and MICAP-setup. If the observed streaks were indeed related to the shimmering of hot gasses, fume extraction would have caused a preferential streak direction, which has not been observed.

Streaks were encountered with and without argon in the outer gas flow. However, the frequency of streaks was rather low for nitrogen as the sole plasma gas (one every few ms) but constantly increased with increasing argon concentration in the

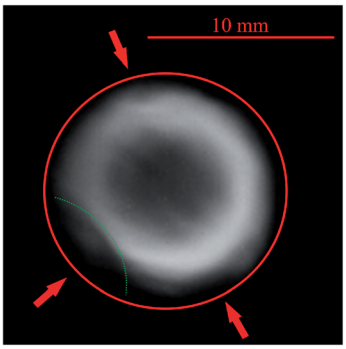

Fig. 6 Single frame from a high-speed video stream (62 μs exposure time) of the MICAP showing plasma streaks (diagonally) passing through the discharge (1000 W microwave power; 0.9 L min^{-1} N_2 nebulizer gas flow, 0.6 L min^{-1} N_2 intermediate gas flow; 14 L min^{-1} outer gas flow with 71% Ar + 29% N_2); please note the pronounced deformation of the plasma discharge highlighted by the red arrows. The red circle has been added as a reference for the inner torch diameter. The green, dotted line highlights one of the streaks warping the plasma torus.

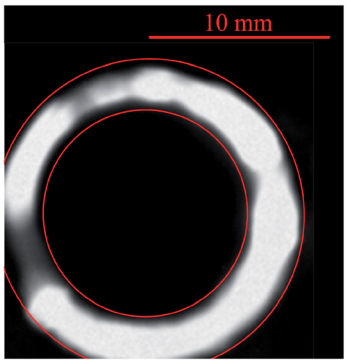

Fig. 7 Single frame from a high-speed video stream (62 μs exposure time) of the filamenting MICAP (1000 W microwave power; 0.9 L min^{-1} N_2 nebulizer gas flow, 0.6 L min^{-1} N_2 intermediate gas flow; 14 L min^{-1} Ar outer gas flow). Red rings have been added to highlight a regular plasma ring.

outer gas flow. At 71% argon in the outer gas stream, always one or more streaks pass through the discharge at a time. It is important to note that these streaks – much like the plasma filaments – appeared randomly around the plasma discharge and no preferential region of creation or preferred orientation was encountered.

The reason for streak-creation remains unclear. The fact that with an increased argon concentration in the outer gas flow the number of streaks increases suggests that there is a connection to the overall gas composition. As noted before, the addition of argon to an initial pure nitrogen plasma will alter the thermal conductivity of the discharge. Consequently, the plasma impedance might change as well. It is interesting to speculate that the resonant nature of a MICAP cavity might be influenced by a plasma impedance other than the tuning impedance of a pure nitrogen plasma. This in turn may cause detuning of the resonant cavity and provokes the increased appearance of streaks. Clearly, a more thorough investigation of this phenomenon is required.

From an analytical point of view, streaks passing through the analyte channel might be expected to cause disturbance of the laminar flow pattern commonly assumed for this region of the plasma. However, no destabilization of the analyte signal indicated by increased RSDs was encountered, even when operating the MICAP with 100% argon in the intermediate- and nebulizer gas flows and 71% argon in the outer gas flow. The reason for this might be the long integration time (24 s) of the ICP-OES spectrometer detectors and the corresponding averaging of the signal. Although no effect of the plasma streaks on the signal stability was encountered for emission spectrometry, they might be of relevance to mass spectrometry, where the dwell time on every m/z is in the millisecond range.

High-speed imaging: plasma filamentation

With increasing argon concentration in the outer gas flow, the MICAP luminous but diffuse plasma core was found to constrict, whereby the analyte channel at the center was widened. When exceeding about 71% argon in the outer gas stream, the diffuse plasma core was found to collapse into a thin, highly luminous ring as shown in Fig. 7. High-speed imaging showed that this ring was in fact formed by several ring segments that were in constant movement. They appeared to rotate around the center of the ring, though their motion seemed to be chaotic. Moreover, segments of low filament luminosity were visible. Also these darker segments followed general rotation and sometimes completely disappeared. A high-speed video showing the filamentation of the MICAP in argon is available(ESI: Plasma_filamentation.mp4).†

From an analytical point of view, the filamented MICAP discharge cannot be expected to be of much use even if the torch damage might be circumvented by an excessively large outer gas flow. As the plasma filament constricts to a thin ring, the energy transfer to the "analyte channel" at the center of this ring can be expected to be poor indeed. This in turn will result in inefficient analyte excitation and severely degraded LODs.

Conclusion

The effect of argon on the analytical performance of a MICAP was found to be small when added either to the nebulizer- or the intermediate gas flow; no effect on the signal intensities of 65 investigated emission lines was encountered when operating the MICAP with 100% argon rather than pure nitrogen in the intermediate gas flow. With the exception of the atom lines of Li, Na, K, P and S, argon caused line-dependent signal suppression when added to the nebulizer gas flow. If, however, nitrogen was replaced by argon in both the nebulizer- and intermediate gas flows, the overall effect was a slight enhancement of most of the investigated emission lines in the range of about 10% to 60%. Consequently, a slight, line energy dependent improvement of LODs was observed, though only for Na(I) 588.995 nm, Na(I) 589.592 nm, Ni(II) 231.604 nm, P(I) 178.287 nm, Sb(I) 206.833 nm, and Sb(I) 217.581 nm a reduction of the LODs by more than a factor of two was encountered.

Consequently, replacing nitrogen with argon in the nebulizer- and intermediate gas flows should be considered if those elements are to be analyzed and lowest possible LODs are of importance.

Argon in the outer gas stream was found to constrict the plasma core resulting in a widening of the analyte cannel by up to 61% of its original surface area. This process was accompanied by a signal suppression of 20 to 50% for all investigated emission lines, with K(I) 766.491 nm being the only exception.

Moreover, the addition of argon to any of the investigated gas streams resulted in no reduction of the highly structured optical plasma background, providing further explanation for the modest overall improvement of the investigated emission line LODs. Based on these findings it can be concluded that the addition of argon to a MICAP presents no significant analytical advantage over a pure nitrogen plasma.

When comparing an argon/nitrogen mixed-gas ICP with a nitrogen/argon mixed-gas MICAP, two distinct differences become obvious; while LODs in ICP-OES[22,23] and ICP-MS[18] in general can be significantly improved by the addition of moderate quantities of nitrogen, the inverse – the addition of argon to an initially all nitrogen MICAP – was shown to degrade LODs at most argon/nitrogen ratios. However, from the plasma stability point of view, the MICAP is far more tolerant to argon, than the ICP is to nitrogen; as shown, argon causes the plasma core of the MICAP to constrict resulting in a widening of the analyte channel. Ultimately, the microwave discharge collapses (filaments). Yet, the fully filamented MICAP discharge remains in the state of a plasma. The ICP on the other hand will extinguish if the concentration of nitrogen in the plasma-forming gas exceeds a certain threshold. It will extinguish because the plasma impedance is vastly altered by the nitrogen and the RF generator ultimately cannot compensate for these changes. While free running RF generators are limited in their allowable frequency response, in crystal controlled RF generators, the impedance matching network will ultimately fail to provide the necessary additional capacitance.

When the concentration of argon in the outer gas flow of a MICAP exceeded about 71%, plasma filamentation – that is the formation of a highly luminous, thin-walled ring discharge – was encountered. The MICAP could not be operated under these conditions over a prolonged time due to the expansion of the plasma towards the quartz torch wall and subsequent damage of the torch (melting).

High-speed imaging showed that the filamented plasma consists of several chaotic rotating segments. For the not filamented, diffuse plasma discharge, high-speed imaging revealed plasma streaks moving at high speed through the discharge. The number of streaks was found to increase with the argon concentration; however they were not found to compromise the signal stability in optical emission spectrometry.

It is interesting to note that depending on the gas composition the plasma robustness changed by up to a factor of two although the excitation temperature remained nearly constant. Moreover, for axial plasma viewing the Mg(II) 280.270 nm/Mg(I) 285.21 nm ratio proved to be a useful parameter for tracking changes in the plasma discharge.

Conflicts of interest

There are no conflicts of interest to declare.

References

1 J. D. Cobine and D. A. Wilbur, The Electronic Torch and Related High Frequency Phenomena, *J. Appl. Phys.*, 1951, **22**, 835–841.
2 M. R. Hammer, A magnetically excited microwave plasma source for atomic emission spectroscopy with performance approaching that of the inductively coupled plasma, *Spectrochim. Acta, Part B*, 2008, **63**, 456–464.
3 H. Wiltsche and M. Wolfgang, Merits of microwave plasmas for optical emission spectrometry – characterization of an axially viewed microwave-sustained, inductively coupled, atmospheric-pressure plasma (MICAP), *J. Anal. At. Spectrom.*, 2020, **35**, 2369–2377.
4 K. J. Jankowski and E. Reszke, *Microwave Induced Plasma Analytical Spectrometry*, Royal Society of Chemistry, Cambridge, 2011.
5 S. Y. Moon, W. Choe, H. S. Uhm, Y. S. Hwang and J. J. Choi, Characteristics of an atmospheric microwave-induced plasma generated in ambient air by an argon discharge excited in an open-ended dielectric discharge tube, *Phys. Plasmas*, 2002, **9**, 4045–4051.
6 Q. Jin, C. Zhu, M. W. Border and G. M. Hieftje, A microwave plasma torch assembly for atomic emission spectrometry, *Spectrochim. Acta, Part B*, 1991, **46**, 417–430.
7 J. H. Barnes IV, O. A. Grøn and G. M. Hieftje, Characterization of an argon microwave plasma torch coupled to a Mattauch–Herzog geometry mass spectrometer, *J. Anal. At. Spectrom.*, 2002, **17**, 1132–1136.
8 Y. Okamoto, M. Yasuda and S. Murayama, High-Power Microwave-Induced Plasma Source for Trace Element Analysis, *Jpn. J. Appl. Phys.*, 1990, **29**, L670–L672.
9 K. Jankowski and A. Jackowska, Spectroscopic diagnostics for evaluation of the analytical potential of argon + helium microwave-induced plasma with solution nebulization, *J. Anal. At. Spectrom.*, 2007, **22**, 1076–1082.
10 K. Jankowski, R. Parosa, A. Ramsza and E. Reszke, Vertically positioned axially viewed aerosol cooled plasma—a new design approach for microwave induced plasma optical spectrometry with solution nebulization, *Spectrochim. Acta, Part B*, 1999, **54**, 515–525.
11 J. Giersz, K. Jankowski, A. Ramsza and E. Reszke, Microwave-driven inductively coupled plasmas for analytical spectroscopy, *Spectrochim. Acta, Part B*, 2018, **147**, 51–58.
12 S. Y. Moon and W. Choe, Parametric study of atmospheric pressure microwave-induced Ar–O_2 plasmas and the ambient air effect on the plasma, *Phys. Plasmas*, 2006, **13**, 103503.
13 R. P. Cardoso, T. Belmonte, C. Noël, F. Kosior and G. Henrion, Filamentation in argon microwave plasma at atmospheric pressure, *J. Appl. Phys.*, 2009, **105**, 093306.
14 Y. C. Hong, H. S. Uhm and S. C. Cho, Argon Microwave Discharges Sustained at Atmospheric Pressure:

Suppression of Plasma Filaments with Molecular Gases, *J. Korean Phys. Soc.*, 2008, **55**, 3220–3223.
15 E. Castaños-Martínez, M. Moisan and Y. Kabouzi, Achieving non-contracted and non-filamentary rare-gas tubular discharges at atmospheric pressure, *J. Phys. D: Appl. Phys.*, 2008, **42**, 012003.
16 H. Louie and S. Y. Soo, Use of N_2 and H_2 in ICP-MS, *J. Anal. At. Spectrom.*, 1992, **7**, 557–564.
17 Z. Hu, S. Gao, Y. Liu, S. Hu, H. Chen and H. Yuan, Signal enhancement in laser ablation ICP-MS by addition of nitrogen in the central channel gas, *J. Anal. At. Spectrom.*, 2008, **23**, 1093–1101.
18 C. Agatemor and D. Beauchemin, Towards the reduction of matrix effects in inductively coupled plasma mass spectrometry without compromising detection limits: The use of argon–nitrogen mixed-gas plasma, *Spectrochim. Acta, Part B*, 2011, **66**, 1–11.
19 A. Montaser and J. Mortazavi, Optical emission spectrometry with an inductively coupled plasma operated in argon–nitrogen atmosphere, *Anal. Chem.*, 1980, **52**, 255–259.
20 S. Greenfield and P. B. Smith, The determination of trace metals in microlitre samples by plasma torch excitation, *Anal. Chim. Acta*, 1972, **59**, 341–348.
21 G. A. Meyer and R. M. Barnes, Analytical inductively coupled nitrogen and air plasmas, *Spectrochim. Acta, Part B*, 1985, **40**, 893–905.
22 M. Ohata, Spectroscopic Characteristic and Analytical Capability of Ar–N_2 Inductively Coupled Plasma in Axially Viewing Optical Emission Spectrometry, *Anal. Sci.*, 2016, **32**, 219–224.
23 G. L. Scheffler and D. Pozebon, Advantages and effects of nitrogen doping into the central channel of plasma in axially viewed-inductively coupled plasma optical emission spectrometry, *Anal. Chim. Acta*, 2013, **789**, 33–40.
24 J. M. Mermet, The use of Mg as a test element for ICP-AES diagnostics, *Anal. Chim. Acta*, 1991, **250**, 85–94.
25 A. J. Schwartz, Y. Cheung, J. Jevtic, V. Pikelja, A. Menon, S. J. Ray and G. M. Hieftje, New inductively coupled plasma for atomic spectrometry: the microwave-sustained, inductively coupled, atmospheric-pressure plasma (MICAP), *J. Anal. At. Spectrom.*, 2016, **31**, 440–449.
26 M. W. Blades, in *Inductively Coupled Plasma Emission Spectroscopy*, ed. P. W. J. M. Boumans, Wiley Interscience, New York, 1987, vol. 90, ch. 11, pp. 387–420.
27 J. R. Fuhr, G. A. Martin, W. L. Wiese and S. M. Younger, Atomic transition probabilities for Fe, Ni, and Co, *J. Phys. Chem. Ref. Data*, 1981, **10**, 305–565.
28 A. N. Zaidel, V. K. Prokofev, S. M. Raiskii, V. A. Slavnyi and E. Y. Shreider, *Tables of spectral lines*, Plenum Press, London, 1970.
29 S. Hesse, T. Ristau and J. W. Einax, Chemical vapor generation by coupling high-pressure liquid flow injection to high-resolution continuum source hydride generation atomic absorption spectrometry for determination of arsenic, *Microchem. J.*, 2015, **123**, 42–50.
30 J. M. Mermet, Ionic to atomic line intensity ratio and residence time in inductively coupled plasma-atomic emission spectrometry, *Spectrochim. Acta, Part B*, 1989, **44**, 1109–1116.
31 N. Chalyavi, P. S. Doidge, R. J. S. Morrison and G. B. Partridge, Fundamental studies of an atmospheric-pressure microwave plasma sustained in nitrogen for atomic emission spectrometry, *J. Anal. At. Spectrom.*, 2017, **32**, 1988–2002.
32 K. M. Thaler, A. J. Schwartz, C. Haisch, R. Niessner and G. M. Hieftje, Preliminary survey of matrix effects in the Microwave-sustained, Inductively Coupled Atmospheric-pressure Plasma (MICAP), *Talanta*, 2018, **180**, 25–31.